

Interplay between potential and spin-flip scattering in systems with depleted density of states

R. G. Dias,¹ Lídia del Rio,² and A. V. Goltsev^{1,3}

¹*Department of Physics and I3N, University of Aveiro, 3810-193 Aveiro, Portugal*

²*Institute for Theoretical Physics, ETH Zurich, 8093 Zurich, Switzerland*

³*A.F. Ioffe Physico-Technical Institute, 194021 St. Petersburg, Russia*

(Received 31 July 2012; published 14 December 2012)

We study the behavior of a magnetic impurity in systems with a depleted density of states by use of the spin-1/2 single-impurity Anderson model and the equation of motion approach. We calculate the impurity spectral function and study the role of potential and spin-flip scattering. We show that in these systems, if the hybridization is larger than a critical value, a narrow virtual bound resonance emerges. The resonance peak appears much below the Fermi energy and is dominated by the contribution of potential scattering of conduction electrons by the magnetic impurity while spin-flip scattering only gives a nonsingular temperature-dependent contribution to this peak. These results are in contrast to behavior of impurities in normal metals where it is spin-flip scattering that is responsible for the Kondo peak near the Fermi level while potential scattering gives a nonsignificant renormalization of the exchange coupling. We also show that the virtual bound resonance leads to a strong renormalization of the effective exchange coupling between conduction and impurity spins. The narrow virtual bound resonance can be observed in graphene with magnetic impurities where its spectral weight and position is strongly influenced by the van Hove singularity.

DOI: [10.1103/PhysRevB.86.235120](https://doi.org/10.1103/PhysRevB.86.235120)

PACS number(s): 72.15.Qm, 75.20.Hr, 72.80.Vp, 71.55.Ak

I. INTRODUCTION

The advent of graphene has renewed the interest in the Kondo effect in systems with depleted density of states (DOS).¹ It is known that a strong depletion of the density of states of a conduction band near the Fermi level modifies the usual behavior of magnetic and nonmagnetic impurities.^{2,3} Impurities in such systems have been addressed, for instance, in the context of d -wave superconductors^{4–6} and more recently graphene,⁷ using a variety of methods, from numerical renormalization group (NRG) approaches^{8–11} to the large N analysis¹² and T -matrix calculations.¹³ The most relevant modification in systems with depleted DOS of the usual Kondo behavior is that the Kondo resonance emerges if the exchange coupling is larger than a critical coupling.^{2,7} Several renormalization group studies, as well as other approaches have addressed this point.^{2,3,7,14–18} These studies have considered a power-law DOS or hybridization function.

Usually, when studying the Kondo effect, it is assumed that potential scattering of conduction electrons on magnetic impurity is not very important and leads only to a renormalization of the density of states near the Fermi level, or equivalently, in a corresponding renormalization of the exchange coupling between localized electron and conduction electrons.¹⁹ It is the assumption that was used in Refs. 2–5 and 7–18. Potential scattering induces a broad peak under the Fermi surface in the conduction band density of states. This peak is known as virtual bound state resonance and can be found by use of the one body approach (see, for example, in Ref. 20 and references therein). In this case, potential scattering does not influence qualitatively the process of the Kondo screening produced by spin-flip scattering of conduction electrons by the magnetic impurity. This has been shown for metals with a sufficiently flat density of states near the Fermi surface.^{19–22} Peaks in the impurity spectral function produced by potential scattering of electrons by impurities were also found in bilayer graphene by Dahal *et al.* using Green's function method.²³ The potential scattering

by a magnetic impurity in d -wave superconductors also gives a noticeable, though weak, contribution to the local density state in the Kondo resonance phase regime.⁶ In contrast to potential scattering, spin-flip scattering results in formation of a narrow resonance peak near the Fermi surface and requires the use of the many-body perturbation theory. The Kondo resonance peak is enhanced with decreasing temperature at the expense of the virtual bound state resonance. In the present paper, we study a single magnetic impurity in a system with depleted DOS using the Anderson model and the equation of motion (EOM) approach, which has been successful in describing the Kondo resonance in systems with a finite density of states at the Fermi level.²⁴ We show that in contrast to the normal metals, in metals with a depleted DOS, a narrow virtual bound state resonance appears under the Fermi surface. This narrow virtual resonance is enhanced with decreasing temperature due to spin-flip scattering, which thus contributes to this peak. Furthermore, this narrow virtual bound resonance leads to strong renormalization of the effective Kondo exchange coupling in the energy range of the Kondo peak. This effect should be taken into account in a renormalization group approach to the Kondo model with depleted density of states. In graphene with a magnetic impurity, we find a similar virtual bound state resonance that depends on temperature. A peculiarity is that the strong van Hove singularity (vHs) in the DOS must be taken into account to for calculating the spectral function of graphene with a magnetic impurity.

II. MODEL

In order to study a magnetic impurity in systems with a depleted DOS, we use the single-impurity Anderson model,

$$H = \sum_{k\sigma} \varepsilon_k \hat{n}_{k\sigma} + \sum_{\sigma} E_0 \hat{n}_{d\sigma} + \frac{1}{2} U \sum_{\sigma} \hat{n}_{d\sigma} \hat{n}_{d\bar{\sigma}} + V \sum_{k\sigma} (c_{k\sigma}^{\dagger} d_{\sigma} + d_{\sigma}^{\dagger} c_{k\sigma}), \quad (1)$$

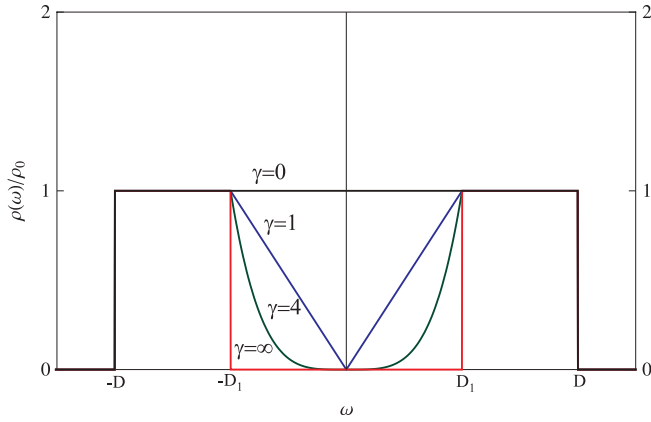


FIG. 1. (Color online) The density of states $\rho(\omega)$ of the conduction band, Eq. (2). The density of states is constant in the energy range $D_1 < |\omega| < D$ and has a power-law dependence $\rho(\omega) = \alpha|\omega|^\gamma$ for $|\omega| < D_1$. The density of states profile for several γ values is displayed. Note that $\gamma = \infty$ implies the existence of a $2D_1$ energy gap.

where the standard notations²⁰ are used: E_0 is the impurity energy level, U is the on-site Coulomb repulsion, and V is the hybridization between conduction and impurity states. This Hamiltonian assumes the isotropic coupling between the impurity and conduction states. In order to describe systems with depleted DOS, we use the following density of states:

$$\rho(\varepsilon) = \begin{cases} \rho_0, & D_1 < |\varepsilon| < D, \\ \rho_0 \left| \frac{\varepsilon}{D_1} \right|^\gamma \equiv \alpha |\varepsilon|^\gamma, & |\varepsilon| < D_1, \end{cases} \quad (2)$$

where $\alpha = \rho_0/D_1^\gamma$ and the Fermi energy is at $\varepsilon_F = 0$. Therefore, $\rho(\varepsilon)$ is zero at the Fermi level. The bandwidth is $2D$. In Fig. 1, the density of states for several values of γ is shown.

Note that this DOS has flat parts outside the interval $D_1 < |\varepsilon| < D$ in contrast to the DOS with the power-law energy dependence in the whole band, $-D < \varepsilon < D$, that was used in Refs. 2–18. The case $\gamma = 1$ corresponds to graphene. However, the van Hove singularities (vHs) in the graphene DOS must also be taken into account to obtain a quantitatively correct spectral function.

III. EQUATION OF MOTION METHOD

The equation of motion approach is basically the successive application of the equation $\omega G_{AB}(\omega) = \langle \{A, B\} \rangle + \langle \langle [A, H]; B \rangle \rangle_\omega$ to the impurity Green's function and to the other Green's function generated in the process.²⁴ Here we adopt the Zubarev notation for the retarded Green's function, $G_{A,B}(\omega) = \langle \langle A; B \rangle \rangle_\omega$.²⁵ As usual, it is implicit that $\omega \rightarrow \omega + i\eta$ where η is a infinitesimal positive constant. In the case of the Anderson model, one obtains the following EOM for the impurity Green's function $\langle \langle d_\sigma; d_\sigma^+ \rangle \rangle$,

$$\left(\omega - E_0 - \sum_k \frac{V^2}{\omega - \varepsilon_k} \right) \langle \langle d_\sigma; d_\sigma^+ \rangle \rangle_\omega = 1 + U \langle \langle \hat{n}_{d\bar{\sigma}} d_\sigma; d_\sigma^+ \rangle \rangle_\omega. \quad (3)$$

In turn, this Green function determines the spectral function

$$A(\omega) = -2 \text{Im} \langle \langle d_\sigma; d_\sigma^+ \rangle \rangle_\omega. \quad (4)$$

If the on-site repulsion between electrons is neglected (i.e., $U = 0$) only potential scattering of conduction electrons contributes to this function. As a result, this equation becomes a closed EOM and leads to

$$\langle \langle d_\sigma; d_\sigma^+ \rangle \rangle_\omega = \frac{1}{\omega - E_0 - \Sigma_0}. \quad (5)$$

The self-energy Σ_0 is

$$\Sigma_0 = \sum_k \frac{V^2}{\omega - \varepsilon_k} = \Lambda_0(\omega) - i\Delta_0(\omega). \quad (6)$$

It can be easily calculated for integer γ . We find

$$\frac{\Delta_0(\omega)}{V^2} = \tau_0(\omega) = \pi\rho(\omega) + \eta, \quad (7)$$

$$\frac{\Lambda_0(\omega)}{V^2} = \lambda_0(\omega) = B(\omega) + P_n(\omega) + \rho_0 \ln \left| \frac{(D+\omega)(D_1-\omega)}{(D-\omega)(D_1+\omega)} \right|, \quad (8)$$

where

$$B(\omega) = \begin{cases} \alpha\omega^\gamma \ln \left| \frac{\omega^2}{D_1^2 - \omega^2} \right|, & \gamma \text{ odd}, \\ \alpha\omega^\gamma \ln \left| \frac{D_1 + \omega}{D_1 - \omega} \right|, & \gamma \text{ even}, \end{cases} \quad (9)$$

and $P_n(\omega)$ is a polynomial of degree $n < \gamma$. In particular cases $\gamma = 1$ and $\gamma = \infty$ (a gapped conduction band), we have $P_n(\omega) = 0$. In Fig. 2, the real part of the self-energy Σ_0 is displayed for $\gamma = 0$, $\gamma = 1$ and $\gamma = \infty$ (the gapped spectrum).

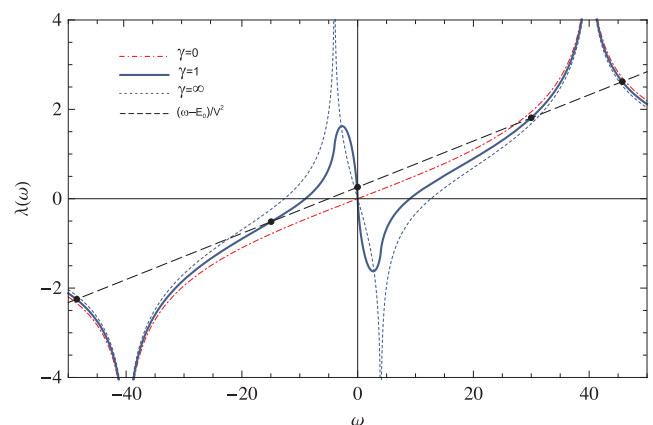


FIG. 2. (Color online) The real part $\lambda_0(\omega)$ of the self-energy Σ_0 , Eq. (8), for the resonant level ($U = 0$) exhibits logarithmic divergences at the band edges and a nonmonotonous behavior in the depletion region. The dashed line represents the line $(\omega - E_0)/V^2$. The black points are the roots of an equation $\lambda_0(\omega) = (\omega - E_0)/V^2$. For $\gamma = \infty$ (the gapped spectrum), additional logarithmic divergences are present at the gap edges. Parameters: $E_0 = -5$, $\rho_0 = 1$, $V = 4.4$, $D_1 = 4$ and $D = 40$.

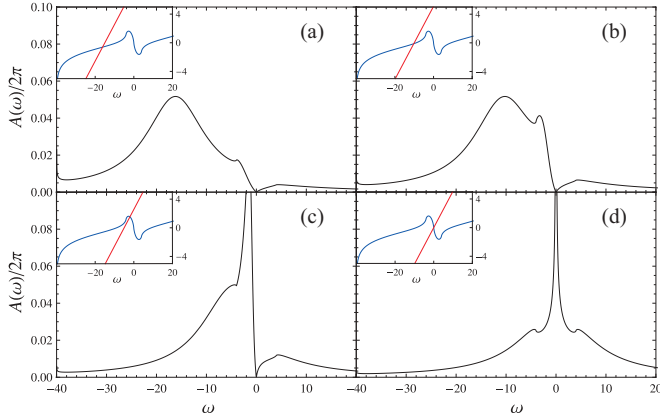


FIG. 3. (Color online) The spectral function $A_0(\omega)$, from Eq. (10), for the resonant level ($U = 0$) for $\gamma = 1$ and several values of the impurity level energy: (a) $E_0 = -15$; (b) $E_0 = -10$; (c) $E_0 = -5$; (d) $E_0 = 0$. Inset: The real part of the self-energy $\lambda_0(\omega)$ and the line $(\omega - E_0)/V^2$. It is the nonmonotonous behavior of $\lambda_0(\omega)$ that generates additional structure in the spectral function for certain intervals of the parameters. For small V , this structure disappears. Other parameters: $\rho_0^{1/2}V = 1.4$, $D_1 = 4$ and $D = 40$.

IV. SPECTRAL FUNCTION AT $U = 0$

In the case $U = 0$, the spectral function $A(\omega)$, Eq. (4) is given by the following function:

$$A_0(\omega) = \frac{2\Delta_0(\omega)}{[\omega - E_0 - \Lambda_0(\omega)]^2 + \Delta_0^2(\omega)} + 2\pi\Theta(D - |\omega|) \sum_i |1 - \Lambda'_0(\omega)|^{-1} \delta(\omega - \omega_i), \quad (10)$$

where ω_i are the roots (outside the band continuum) of an equation,

$$\text{Re}[\langle\langle d_\sigma; d_\sigma^+ \rangle\rangle_\omega^{-1}] = 0, \quad (11)$$

which takes a form $\omega - E_0 - \Lambda_0(\omega) = 0$. According to Eq. (10), the function $A_0(\omega)$ exhibits the same behavior at the Fermi level as the density of states in Eq. (2) [i.e., $A_0(\omega) \propto |\omega|^\gamma$ and $A_0(0) = 0$]. Figure 3 represents the spectral function $A_0(\omega)$ for different impurity levels E_0 .

One can see that, apart from a broad peak that also takes place in normal metals, an additional narrow virtual bound resonance appears within the depleted region. The positions of these peaks are given by Eq. (11). Analysis of Eq. (11) shows that this additional narrow peak appears due to the fact that the self-energy Σ_0 has a peak (see insets in Fig. 3), which is absent in normal metals. The narrow peak strongly depends on the hybridization V and the impurity level energy E_0 . At a given E_0 , there is a critical hybridization V_c [see Fig. 3(c)] above which the maximum of this narrow peak becomes so large that it actually looks like a Kondo resonance. The critical hybridization V_c can be found as a value of V at which the line $(\omega - E_0)/V^2$ in Fig. 3 touches the peak of the self-energy $\lambda_0(\omega)$, see Eq. (21) below. Alternatively, at a given hybridization V , this narrow resonance appears when the impurity level E_0 is larger than a critical energy

at which the line touches the peak of $\lambda_0(\omega)$ (the critical energy is approximately -6 for the parameters in Fig. 3). When the impurity level E_0 moves closer to the Fermi energy, the additional resonance peak also moves closer to the Fermi energy and its width decreases. It is necessary to outline that this narrow peak is due to potential scattering of conduction electrons by the impurity and does not depend on temperature.

V. SPECTRAL FUNCTION AT $U \neq 0$

Now we consider the case $U \neq 0$ and take into account the last term in Eq. (3) that allows us to take into account many-body interactions due to spin-flip scattering of conduction electrons off the impurity spin. Using the Appelbaum and Penn approximation,²⁶ we find the following expression for the impurity Green's function for $U = \infty$,

$$\begin{aligned} & (\omega - E_0 - \Sigma) \langle\langle d_\sigma; d_\sigma^+ \rangle\rangle_\omega \\ &= 1 - \langle n_{d\bar{\sigma}} \rangle - V \sum_k \frac{\langle d_\sigma^+ c_{k\bar{\sigma}} \rangle}{\omega - \varepsilon_k}, \end{aligned} \quad (12)$$

where $\Sigma = \Sigma_0 + \Sigma_1 + \Sigma_2$,

$$\Sigma_1 = V^2 \sum_{k,k'} \frac{\langle c_{k'\bar{\sigma}}^+ c_{k\bar{\sigma}} \rangle}{\omega - \varepsilon_k}, \quad (13)$$

$$\Sigma_2 = -V^3 \sum_{k,k'} \frac{\langle d_\sigma^+ c_{k\bar{\sigma}} \rangle}{(\omega - \varepsilon_k)(\omega - \varepsilon_{k'})}, \quad (14)$$

and Σ_0 is given by Eq. (6). In contrast to Σ_0 , the contributions of spin-flip scattering represented by Σ_1 and Σ_2 have a strong temperature dependence. This dependence can be analyzed analytically at sufficiently small V when the self-energy Σ_2 can be neglected [however, in our numerical solution of Eq. (12) discussed below, the self-energy Σ_2 is taken into account]. In this case, the temperature behavior of the spectral function is determined by Σ_1 that is approximately given by

$$\begin{aligned} \frac{\Sigma_1(\omega, T)}{V^2} &= i\tau_1(\omega, T) + \lambda_1(\omega, T) \\ &\approx -i\pi\rho(\omega)f(\omega) \\ &\quad + \int d\omega' \rho(\omega')f(\omega')P\left(\frac{1}{\omega - \omega'}\right). \end{aligned} \quad (15)$$

where $f(x)$ is the Fermi-Dirac distribution function. The temperature dependence can be found in an explicit form at $\gamma = 1$ and $k_B T < D_1$,

$$\begin{aligned} \lambda_1(\omega, T) &\approx \rho_0 \ln \left| \frac{D + \omega}{D_1 + \omega} \right| + \alpha(D_1 - k_B T) \\ &\quad + \alpha\omega \ln \frac{\sqrt{\omega^2 + (ak_B T)^2}}{|D_1 + \omega|}, \end{aligned} \quad (16)$$

where $\alpha \sim \pi$. Note that the function $\text{Re}[\Sigma_1(\omega)]$ in Eq. (16) is finite at the Fermi energy $\omega = \varepsilon_F = 0$ even in the limit $T \rightarrow 0$. This energy and temperature behavior of $\text{Re}[\Sigma_1(\omega)]$ is also valid in a general case $\gamma > 1$.

As above, Eq. (11) determines peaks in the energy dependence of the spectral function $A(\omega)$ at energies given by

$$\omega - E_0 - \text{Re}(\Sigma_0 + \Sigma_1) = 0. \quad (17)$$

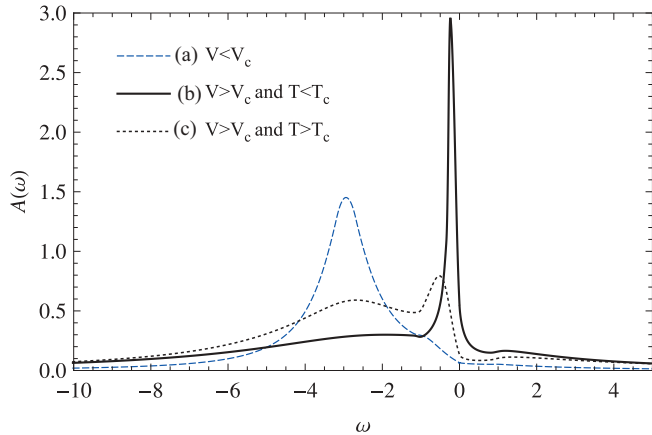


FIG. 4. (Color online) The spectral function $A(\omega)$, for $U = \infty$, $\gamma = 1$, and several values of the hybridization V . Curve (a) displays the typical $V < V_c$ spectral function characterized by the absence of a Kondo resonance. The Kondo peak appears as V is increased above a critical value V_c [curve (b)] and disappears above the Kondo temperature T_c [curve (c)]. Other parameters: $E_0 = -3.2$, $\rho_0 = 10$, $D_1 = 1$, $D = 20$ and (a) $V = 0.12$, $k_B T = 0.05$; (b) $V = 0.24$, $k_B T = 0.05$; (c) $V = 0.24$, $k_B T = 10$.

The self-energy $\Sigma = \Sigma_0 + \Sigma_1$ has two contributions. First, a temperature-independent term due to potential scattering and, second, a temperature-dependent term due to spin-flip scattering. Analyzing Eqs. (8) and (15), we find that the function $\text{Re}[\Sigma_0(\omega) + \Sigma_1(\omega)]$ has a peak that at all T is placed in the depleted energy range $-D_1 < \omega < 0$. Thus, we meet situations that are qualitatively similar to one shown in Fig. 3 when only $\text{Re}[\Sigma_0(\omega)]$ (i.e., potential scattering alone) is taken into account. Our results are represented in Figs. 4 and 5. One sees that apart from a broad peak there is a narrow peak in the depleted region. In contrast to Fig. 3, the narrow virtual bound resonance peak depends on temperature due to the spin-flip scattering contribution $\Sigma_1(\omega)$. In the case of a strong depletion of the density of states [i.e., ($\gamma \gg 1$) in Eq. (2)] the narrow

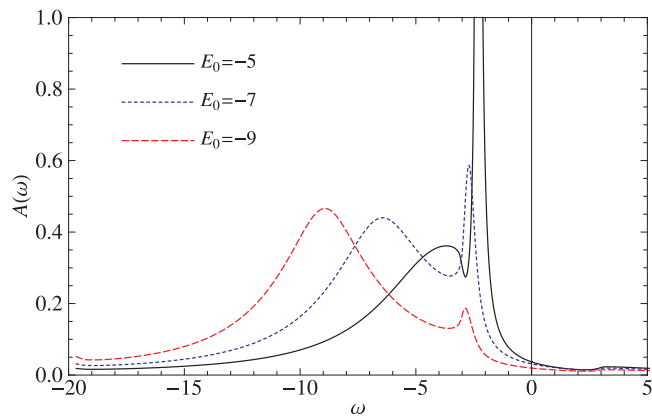


FIG. 5. (Color online) The spectral function $A(\omega)$ for $U = \infty$, $\gamma = 8$, and several values of the impurity energy, $E_0 = -5, -7$, and -9 . One can see that when E_0 increases and approaches the edge of the depletion region ($\omega = -3$, on this figure), the Kondo peak grows within the depletion region much below the Fermi energy. Other parameters: $\rho_0 = 10$, $D_1 = 3$, $D = 20$, $V = 0.2$, and $k_B T = 0.05$.

virtual bound resonance peak grows and approaches the lower edge $-D_1$ of the depletion region (see Fig. 5).

VI. CRITICAL HYBRIDIZATION FOR THE VIRTUAL BOUND RESONANCE

For better understanding of the origin of the narrow virtual bound resonance peak, we compare it with the Kondo resonance in normal metals. In the case of a flat DOS, the Lacroix approach²⁴ leads to the function

$$\lambda_1(\omega, T) \approx -\rho_0 \ln[\sqrt{\omega^2 + (\pi k_B T)^2}/D]. \quad (18)$$

This function diverges when $\omega \rightarrow 0$ at $T = 0$ in contrast to $\text{Re}[\Sigma_0(\omega)]$, which goes to zero at $\omega \rightarrow 0$. Thus at low temperatures, the self-energy $\text{Re}[\Sigma_0(\omega) + \Sigma_1(\omega)]$ has a narrow peak only due to $\text{Re}[\Sigma_1(\omega)]$. As a result, there is a critical temperature T_K at which Eq. (17) has an additional solution at energy ω near the Fermi level $\varepsilon_F = 0$ apart from a solution corresponding to a broad virtual bound resonance at an energy far below the Fermi surface. This additional solution appears when the line $\omega - E_0$ touches the maximum of $\text{Re}(\Sigma_0 + \Sigma_1)$. Therefore, we arrive at the condition $E_0 = \rho_0 V^2 \ln(k_B T_K/D)$, which determines the Kondo temperature and has a solution for any value of V , however small it may be, due to the logarithmic dependence on temperature.

Now we find the critical hybridization V_c at which a narrow virtual resonance appears. According to Eq. (17), we should find a hybridization at which the line $\omega - E_0$ touches the maximum of $\text{Re}[\Sigma_1(\omega, 0) + \Sigma_0(\omega)]$. At large γ , the function $\lambda_1(\omega, 0)$ can be found analytically from Eq. (15) at ω near the boundary of the depleted region, $\omega = -D_1$,

$$\begin{aligned} \lambda_1(\omega, 0) \approx & \rho_0 \ln \left| \frac{D + \omega}{D_1 + \omega} \right| + \alpha D_1^\gamma \\ & + \alpha D_1^\gamma \left[1 - \gamma \left(1 + \frac{\omega}{D_1} \right) \right] \ln \left| 1 - \frac{1/\gamma}{1 + \frac{\omega}{D_1}} \right|. \end{aligned} \quad (19)$$

In the case $D = D_1$, this function has a maximum at $\omega_{\max} \approx -D_1 + 3D_1/4\gamma$ and, therefore, $\lambda_1(\omega_{\max}, 0) \approx \rho_0$. In the case $D \gg D_1$, the maximum of λ_1 is at $\omega_{\max} \approx -D_1 + D_1/a\gamma$ (where a is a constant of the order of 1) and $\lambda_1(\omega_{\max}, 0) \approx \rho_0 \ln(a\gamma D/D_1)$.

If $E_0 \lesssim -D_1$ and $\gamma \gtrsim 1$, then, using Eqs. (8) and (9) for $\Sigma_0(\omega)$ and Eq. (20) for $\Sigma_1(\omega)$, we find that the maximum of $\text{Re}[\Sigma_0(\omega) + \Sigma_1(\omega, 0)]$ occurs at ω_{\max} found above. As a result, V_c is given by an equation,

$$\begin{aligned} \frac{\omega_{\max} - E_0}{V_c^2} & \approx \max(\lambda_1 + \lambda_0) \\ & \sim \begin{cases} \alpha D_1^\gamma \ln(a\gamma^2 D/D_1), & D \gg D_1, \\ 2\alpha D_1^\gamma, & D = D_1. \end{cases} \end{aligned} \quad (20)$$

In the case $U = 0$, one obtains a similar result,

$$\frac{\omega_{\max} - E_0}{V_c^2} \approx \lambda_0^{\max} \sim \begin{cases} \alpha D_1^\gamma \ln(\gamma), & D \gg D_1, \\ \alpha D_1^\gamma, & D = D_1. \end{cases} \quad (21)$$

Equations (20) and (21) for $D \gg D_1$ shows that with increasing γ (i.e., with increasing the depletion of the DOS) the energy of the narrow virtual bound resonance is gradually

shifted from the Fermi level to the lower boundary of the depleted region (see Fig. 5) and in the strong depletion limit $\gamma \gg 1$, the peak in the impurity spectral function exists at any value of the hybridization since λ_0^{\max} diverges logarithmically as $\gamma \rightarrow \infty$. In the particular case of a hard-gap density of states (i.e., $\gamma \gg 1$) this peak looks like a subgap Dirac δ function, which is placed near the lower gap edge. In superconducting systems, similar subgap peaks near the upper and lower gap edges were found by use of different methods. For example, subgap resonances in the impurity spectral function in s -wave superconducting systems with a single Anderson impurity were found by use of the NRG method.^{27,28} These subgap peaks are associated with Andreev bound states. The NCA and EOM approaches in Refs. 29 and 30 give similar results. Though an explicit analytical expression for the critical temperature T_K is unknown for an arbitrary exponent γ , this critical parameter can be found numerically, using the following method. Decrease temperature starting from a high-temperature region. T_K can be found as a temperature at which the peak of the real part of the self-energy $\Sigma \approx \Sigma_0 + \Sigma_1$ touches the line $\omega - E_0$.

VII. MAGNETIC IMPURITY IN GRAPHENE

Graphene is particular within the gapless systems universe since the depleted region in the DOS is wide and framed by the van Hove singularity (vHs) (see the inset in Fig. 6). It has been shown that, in metals, if the van Hove singularity (vHs) (with a logarithmic divergence of the DOS) is pinned at the Fermi level, then the Kondo resonance is enhanced due to a zero-frequency log-squared divergence of the real part of the self-energy.³¹ However, if the vHS is shifted from the Fermi level (without depletion of the DOS), the usual log divergence due to Kondo effect is recovered and the vHs singularity is only signaled by a steplike feature in the real part of the self-energy.

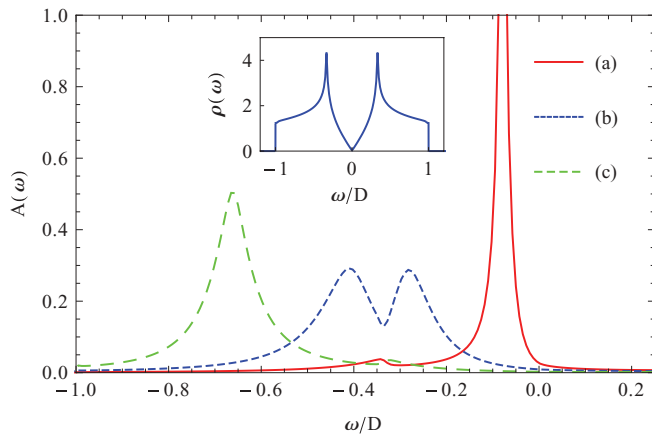


FIG. 6. (Color online) The spectral function $A(\omega)$ of graphene in the case $U = \infty$ at several values of the impurity energy E_0 : (a) $E_0/D = -0.125$ above the van Hove singularity (vHs) (red solid line); (b) $E_0/D = -0.375$ at the vHs (blue short dashed line); (c) $E_0/D = -0.625$ below the vHs (green dashed line). Note that the spectral weight of the narrow virtual bound resonance peak in the vicinity of the vHs is strongly reduced if the impurity level is below but near the vHs. Inset: the DOS of graphene. Other parameters: $V/D = 0.0125$, and $k_B T/D = 2.5 \times 10^{-4}$.

Using Eqs. (12)–(14) and the DOS of graphene from Ref. 32 (see inset in Fig. 6), we calculated numerically the spectral function of graphene with a magnetic impurity. This approach enabled us to take into account both potential and spin-flip scattering, and the van Hove singularity. However, note that this approach uses the Hamiltonian Eq. (1) with the isotropic coupling between conduction and impurity states and neglects umklapp scattering processes. We found that the vHs leads to a similar steplike feature in self-energy $\text{Re}[\Sigma_0(\omega) + \Sigma_1(\omega)]$ at the vHs energy and a broadening of the virtual bound resonance peak discussed in the previous sections. More importantly, the vHs leads to a large imaginary part of the self-energy near the vHs energy. This effect strongly reduces the spectral weight of the narrow virtual peak in the vicinity of the vHs and leads to a spectral profile with two broad peaks if the impurity level is below but near the vHs (see Fig. 6). This reduction can be explained by the fact that potential scattering is screened stronger in the energy region with large density of states (i.e., at the van Hove singularity). Despite these effects produced by the vHs, the spectral function of graphene with a magnetic impurity demonstrates a narrow virtual bound resonance similar to one we found in Secs. IV–VI for other systems with depleted DOS. A virtual bound resonance produced by potential scattering of electrons by impurities was also found in bilayer graphene by Dahal *et al.*²³ Unfortunately, spin-flip scattering of electrons by magnetic impurities was not yet considered for this material.

VIII. RENORMALIZATION OF EXCHANGE COUPLING

Above we applied perturbation theory to the Anderson model and found contributions of potential and spin-flip scattering to the impurity spectral function. Alternatively, at first one can find an exchange interaction between spins of conduction electrons and the impurity. Then, one can calculate a contribution of this interaction to the spectral function. In this case, the standard way is to apply a canonical transformation to the Anderson model.^{20,21} However, this transformation generates not only the s - d exchange interaction but also a potential term that describes scattering of conduction electrons off the impurity. In the case of $U = \infty$, the amplitude $K_{\mathbf{k},\mathbf{k}'}$ of scattering from a state with momentum \mathbf{k} to a state with momentum \mathbf{k}' is $K_{\mathbf{k},\mathbf{k}'} = 1/2V^2/(\epsilon_{\mathbf{k}} - E_0)$.^{20,21} This potential term can be eliminated from the effective Hamiltonian by use of a unitary transformation, which in turn modifies the exchange coupling.^{19,21,22} As a result, the renormalized exchange coupling is given by an equation,¹⁹

$$\tilde{J}(\omega) \approx \frac{J}{|1 - K(\omega)\Sigma_0(\omega)/V^2|^2} \quad (22)$$

$$\approx J \cdot \frac{|\omega - E_0|^2}{2\Delta_0(\omega)} A_0(\omega), \quad (23)$$

where $K(\omega)$ is the scattering amplitude at $\epsilon_{\mathbf{k}} = \omega$. Here we dropped a factor 2, which does not affect qualitatively our conclusions. In the case of normal metals with a flat band, the renormalization factor in Eq. (23) has a weak energy dependence. The real part of the self-energy Σ_0 is small in the frequency range of the Kondo resonance (i.e., near the Fermi level) and only the imaginary part $\Sigma_0(\epsilon_F) \approx -i\pi\rho_0V^2$

is important. This leads to the well-known result,^{19,21}

$$\tilde{J}(\epsilon_F) \approx J/[1 + (\pi\rho_0 V^2/E_0)^2]. \quad (24)$$

However, in the case of the depleted density of states, Eq. (23), such approximation is not valid in the frequency range of the narrow virtual bound resonance because $A_0(\omega)$ has a sharp maximum [see Fig. 3(c)]. Thus, in the range of the virtual resonance in systems with a depleted DOS, a strong enhancement of the effective exchange coupling $\tilde{J}(\omega)$, Eq. (24), occurs in contrast to the small reduction of the exchange coupling, Eq. (24), in normal metals.

IX. CONCLUSION

In conclusion, we calculated the spectral function of magnetic impurities in a gapless system with a depleted density of states (DOS) about the Fermi level. For this purpose, we used the equation of motion approach that allowed us to take into account both potential scattering of conduction electrons by magnetic impurities and many-body interactions between conduction electrons and magnetic impurities due to multiple spin-flip scattering processes. We found that a depletion of the DOS results in the enhancement of the role of potential scattering of conduction electrons by magnetic impurities. We revealed that the potential scattering produces a narrow virtual bound resonance peak below the Fermi level in the spectral function. The peak is strongly enhanced if the

hybridization (or the impurity energy) between the conduction and impurity electron states is larger than a critical value. Furthermore, potential scattering strongly renormalizes the exchange interaction between spins of conduction electrons and magnetic impurities. Spin-flip scattering only gives a temperature-dependent contribution that has no singularity even at zero temperature. Our results are in contrast to behavior of magnetic impurities in normal metals with a finite DOS at the Fermi level where it is spin-flip scattering that leads to the narrow Kondo peak near the Fermi level while potential scattering produces only a small renormalization of the DOS at Fermi level and a small reduction of the exchange coupling between spins of conduction and impurity electrons. We also calculated the spectral function of graphene with a magnetic impurity. We found that besides the phenomena described above, the van Hove singularities in this material are also important and influence on the position and the spectral weight of the virtual bound resonance peak. The peculiarities of the impurity spectral function found in the present paper could be observed by use of the usual experimental probes of the Kondo effect such as the scanning tunneling microscopy³³ or conductance measurements in quantum dot devices with semimetallic leads.³⁴ Our results on the interplay between potential and spin-flip scattering by magnetic ions may also be useful for understanding heavy-fermion compounds such as iron arsenides, which have a partially depleted density of electron states at the Fermi level.³⁵

¹A. H. C. Neto, F. Guinea, N. M. R. Peres, K. S. Novoselov, and A. K. Geim, *Rev. Mod. Phys.* **81**, 109 (2009).

²D. Withoff and E. Fradkin, *Phys. Rev. Lett.* **64**, 1835 (1990).

³K. Ingersent, *Phys. Rev. B* **54**, 11936 (1996).

⁴A. Polkovnikov, S. Sachdev, and M. Vojta, *Phys. Rev. Lett.* **86**, 296 (2001).

⁵M. Vojta and R. Bulla, *Phys. Rev. B* **65**, 014511 (2001).

⁶J. X. Zhu and C. S. Ting, *Phys. Rev. B* **63**, 020506 (2000).

⁷K. Sengupta and G. Baskaran, *Phys. Rev. B* **77**, 045417 (2008).

⁸R. Bulla, T. Pruschke, and A. C. Hewson, *J. Phys.: Condens. Matter* **9**, 10463 (1997).

⁹L. Fritz and M. Vojta, *Phys. Rev. B* **72**, 212510 (2005).

¹⁰C. Gonzalez-Buxton and K. Ingersent, *Phys. Rev. B* **57**, 14254 (1998).

¹¹C. Gonzalez-Buxton and K. Ingersent, *Phys. Rev. B* **54**, 15614 (1996).

¹²A. Polkovnikov, *Phys. Rev. B* **65**, 064503 (2002).

¹³A. V. Balatsky, I. Vekhter, and J. X. Zhu, *Rev. Mod. Phys.* **78**, 373 (2006).

¹⁴M. Glossop and D. Logan, *Eur. Phys. J. B* **13**, 513 (2000).

¹⁵M. T. Glossop, G. E. Jones, and D. E. Logan, *J. Phys. Chem. B* **109**, 6564 (2005).

¹⁶M. T. Glossop and D. E. Logan, *J. Phys.: Condens. Matter* **15**, 7519 (2003).

¹⁷D. E. Logan and M. T. Glossop, *J. Phys.: Condens. Matter* **12**, 985 (2000).

¹⁸R. Bulla, M. T. Glossop, D. E. Logan, and T. Pruschke, *J. Phys.: Condens. Matter* **12**, 4899 (2000).

¹⁹J. Kondo, *Phys. Rev.* **169**, 437 (1968).

²⁰A. Hewson, *The Kondo Problem to Heavy Fermions* (Cambridge University Press, Cambridge, 1993).

²¹J. R. Schrieffer and P. A. Wolff, *Phys. Rev.* **149**, 491 (1966).

²²K. Fischer, *Phys. Rev.* **158**, 613 (1967).

²³H. P. Dahal, A. V. Balatsky, and J.-X. Zhu, *Phys. Rev. B* **77**, 115114 (2008).

²⁴C. Lacroix, *J. Phys. F* **11**, 2389 (1981).

²⁵D. Zubarev, *Sov. Phys. Usp.* **3**, 320 (1960).

²⁶J. A. Appelbaum and D. R. Penn, *Phys. Rev.* **188**, 874 (1969).

²⁷T. Hecht, A. Weichselbaum, J. von Delft, and R. Bulla, *J. Phys.: Condens. Matter* **20**, 275213 (2008).

²⁸J. Bauer, A. Oguri, and A. C. Hewson, *J. Phys.: Condens. Matter* **19**, 486211 (2007).

²⁹M. Krawiec and K. I. Wysokinski, *Supercond. Sci. Technol.* **17**, 103 (2004).

³⁰A. A. Clerk, V. Ambegaokar, and S. Hershfield, *Phys. Rev. B* **61**, 3555 (2000).

³¹A. O. Gogolin, *Z. Phys. B* **92**, 55 (1993).

³²P. R. Wallace, *Phys. Rev.* **71**, 622 (1947).

³³H. Manoharan, C. Lutz, and D. Eigler, *Nature (London)* **403**, 512 (2000).

³⁴D. Goldhaber-Gordon, H. Shtrikman, D. Mahalu, D. Abusch-Magder, U. Meirav, and M. A. Kastner, *Nature (London)* **391**, 156 (1998).

³⁵J. Dai, J.-X. Zhu, and Q. Si, *Phys. Rev. B* **80**, 020505 (2009).